

An Apparent Angle Dependence for the Nonradiative Deactivation of Excited Triplet States of Sterically Constrained, Binuclear Ruthenium(II) Bis(2,2':6',2''-terpyridine) Complexes

Andrew C. Benniston, Anthony Harriman,* Peiyi Li, Pritesh V. Patel, James P. Rostron, and Craig A. Sams

Molecular Photonics Laboratory, School of Natural Sciences, Bedson Building, University of Newcastle, Newcastle upon Tyne, NE1 7RU, U.K.

Received: February 19, 2006; In Final Form: June 14, 2006

The photophysical properties are reported for a series of binuclear ruthenium(II) bis(2,2':6',2''-terpyridine) complexes built around a geometrically constrained, biphenyl-based bridge. The luminescence quantum yield and lifetime increase progressively with decreasing temperature, but the derived rate constant for nonradiative decay of the lowest-energy triplet state depends on the length of a tethering strap attached at the 2,2'-positions of the biphenyl unit. Since the length of the strap determines the dihedral angle for the central C–C bond, the rate of nonradiative decay shows a pronounced dependence on angle. The minimum rate of nonradiative decay occurs when the dihedral angle is 90°, but there is a maximum in the rate when the dihedral angle is about 45°. This effect does not appear to be related to the extent of electron delocalization at the triplet level but can be explained in terms of variable coupling with a low-frequency vibrational mode associated with the strapped biphenyl unit.

Introduction

The rates of decay of the lowest-energy, excited triplet states of many transition metal complexes are controlled by the Englman–Jortner energy-gap law.^{1,2} Within the framework of this theory, the rate of decay can be considered in terms of the amount of electronic energy to be dissipated³ and the nature of the dissipating vibrational mode.⁴ A key element in this model is the vibrational–electronic coupling matrix element that describes the extent of interaction between the excited state and high vibrational levels of the ground state. Detailed analysis of kinetic data in terms of the energy-gap law has been made for numerous compounds⁵ but is often complicated by the presence of thermally activated processes.⁶ This is particularly evident for ruthenium(II) poly(pyridine) complexes where the lowest-energy triplet state couples to at least two higher-energy excited states.⁷ In certain cases, the situation is further exacerbated by the appearance of hot emission from thermally accessible upper-lying excited states.⁸

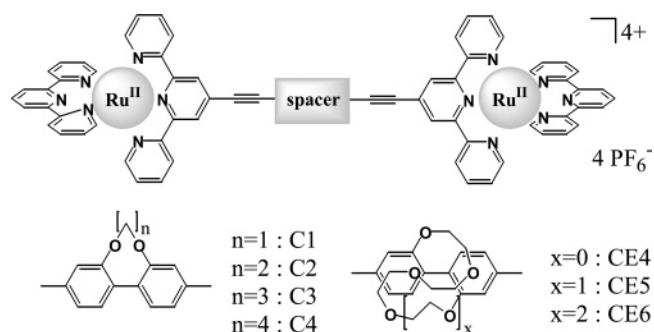
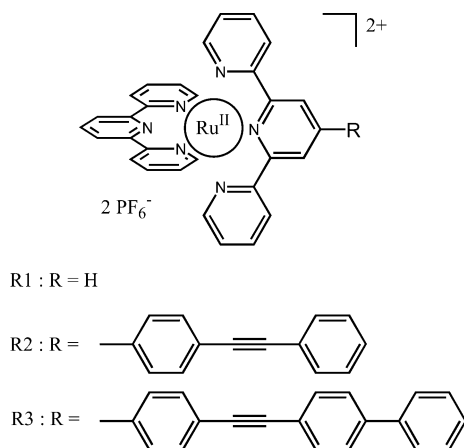
Where the lowest-energy excited triplet state is of metal-to-ligand, charge-transfer (MLCT) character, there exists the possibility to delocalize the promoted electron over part of an extended π -conjugated ligand.⁹ This effect, which has been reported for numerous systems,¹⁰ can be explained within the energy-gap law in terms of a decreased nuclear displacement. In principle, the concept of extended electron delocalization could be exploited to design luminophores with prolonged triplet lifetimes, a highly desirable feature for chemical sensors. Systematic examination of the effect of incremental degrees of electron delocalization, however, is rendered difficult by the nonavailability of suitable probe molecules. This restriction, together with the onset of thermally activated decay routes, means that the electron delocalization effect is still not properly understood.

Previously, we reported¹¹ that the photophysical properties of a set of binuclear ruthenium(II) bis(2,2':6',2''-terpyridine) complexes were dependent on the conformation of the bridging unit. The only obvious structural change among these complexes concerns the variation in dihedral angle for the central C–C bond of the biphenyl-based connector. At first sight, this observation raises the possibility that the degree of electron delocalization at the triplet level might be set by the conformation of the biphenyl linker.¹² This, in turn, would introduce an angle dependence for the rate of nonradiative decay of the lowest-energy triplet state. This series of compounds has been expanded from four to eleven, and a full investigation of their photophysical properties has been completed. It is confirmed that the lifetime of the emitting triplet state depends on the central dihedral angle of the bridging biphenyl unit, with a clear maximum in the rate constant when the dihedral angle is held around 45°. This effect is believed to arise from increased coupling of a low-frequency vibrational mode.

Experimental Section

The synthesis¹³ and characterization of the various binuclear ruthenium(II) bis(2,2':6',2''-terpyridine) complexes will be reported in full elsewhere. The molecular formulas and abbreviations used for these compounds are shown in Chart 1 while the ability of the crown ethers to bind adventitious cations has been described for simpler molecular analogues.¹⁴ Preliminary photophysical data were provided before for some members of the series,¹¹ and their electrochemical properties were described as part of an investigation into the behavior of the corresponding mixed-valence compounds.¹⁵ Details regarding the synthesis of **R3** (Chart 2) are provided as part of the Supporting Information. Butyronitrile was purchased from Aldrich and redistilled from CaH₂. A sample was freshly distilled immediately before use. Samples of the cation (M = Li⁺, Na⁺, K⁺) complexes were obtained by adding a large excess of perchlorate salt to the sample solution. Electro spray

* Author to whom correspondence should be addressed. E-mail: anthony.harriman@ncl.ac.uk. Tel and fax: +44 (0)191 222 8660.

CHART 1. Molecular Formulas and Abbreviations Used for the Compounds Studied Herein**CHART 2. Structural Formulas for the Reference Compounds Used Herein**

mass spectrometry confirmed cation binding under these conditions. Absorption spectra were recorded with a Hitachi U3310 spectrophotometer, and emission spectra were recorded with a Jobin-Yvon Fluorolog tau-3 spectrofluorimeter. Emission spectra were corrected for spectral imperfections by reference to a standard lamp. Spectra were recorded for dilute samples, absorbance less than 0.15 at 500 nm, after deoxygenation and sealing into optical cells. Luminescence quantum yields were measured by reference to osmium(II) bis(2,2':6',2''-terpyridine).¹⁶ Temperature dependence studies were made with an Oxford Instruments Optistat DN cryostat. Time-resolved emission spectra were recorded by time-correlated, single-photon counting methods following excitation at 490 nm with a laser diode (fwhm = 90 ps). Transient absorption spectra were recorded with an Applied Photophysics LNS-60 laser flash spectrometer (fwhm = 4 ns; $\lambda = 532$ nm). The monitoring beam was provided with a pulsed xenon arc lamp and detected with a PMT after passage through a high radiance monochromator. At least 25 individual laser shots were averaged for kinetic measurements.

Data analysis was made as described before.¹⁷ The reduced emission spectra were deconvoluted into the minimum number of Gaussian-shaped components, of common half-width, needed to give a good representation of the full spectrum.¹⁸ This procedure was repeated across the entire temperature range. According to this analysis, the position in wavenumbers (cm^{-1}) of the highest-energy Gaussian component, E_{00} , is taken to represent the energy gap between 0,0 vibrational levels in the ground and excited states while the spacing between Gaussian peaks refers to the vibrational mode coupled to nonradiative decay of the excited triplet state. Even in fluid solution, it was necessary to include both medium- and low-frequency vibra-

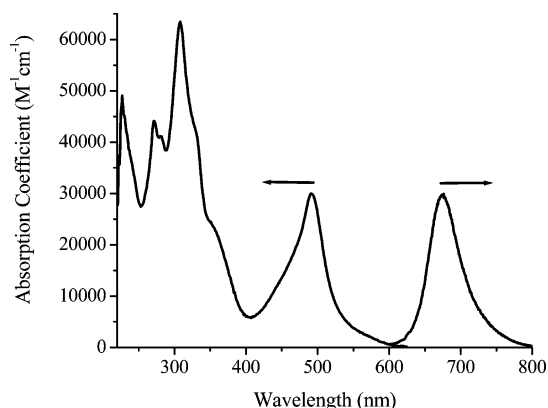


Figure 1. Absorption and emission spectral profiles recorded for **CE4** in deoxygenated butyronitrile at 20 °C.

tional bands to obtain a proper fit to the emission spectrum.⁸ The full-width at half-maximum (fwhm) of the Gaussian components provides a measure of the reorganization energy that accompanies deactivation of the triplet state, but the experimental value is instrumentally broadened at high temperature. As such, the fwhm was measured over a wide temperature range and used to derive the corrected reorganization energy for each compound. An illustration of this analytical protocol is provided as part of the Supporting Information. The derived parameters were used to reconstitute the full emission spectrum, as described in the text, in order to obtain a value for the Huang–Rhys factor.¹⁹

Results and Discussion

General Spectroscopic Features. The absorption spectrum recorded for each member of the series contains several easily recognizable features (Figure 1). Thus, the capping terpy ligands absorb around 290 nm while the ditopic bridging ligand displays pronounced absorption between 300 and 400 nm. The [nominally] spin-allowed MLCT transition is centered at about 500 nm, with the [nominally] spin-forbidden MLCT transition stretching toward 620 nm. The nature of the tethering strap has no effect on the position or intensity of these absorption bands. Weak emission can be observed around 675 nm (Figure 1), in each case, in deoxygenated butyronitrile at room temperature. The corrected excitation spectrum matches with the absorption spectrum over the entire visible and near-UV regions, and the emission intensity is decreased slightly upon aeration of the solution. For each compound, the emission quantum yield (Φ_{LUM}) is of the order of about 0.0005 while the excited-state lifetime (τ_{LUM}) is about 20 ns. Decay of the luminescence signal followed first-order kinetics. The same lifetime was obtained by laser flash photolysis methodology after excitation at 532 nm. As above, the nature of the strap has no significant effect on the photophysical properties recorded at room temperature. In all cases, the emitting species could be assigned to the lowest-energy MLCT triplet state by reference to earlier work with related compounds.²⁰ The observed Φ_{LUM} and τ_{LUM} values are within the range expected for ethynylated Ru-terpy derivatives.²¹ Suitable reference compounds include the parent complex (**R1**), a phenylethyne derivative (**R2**), and the corresponding biphenylethyne derivative (**R3**), as shown in Chart 2.

Derivation of the Nonradiative Rate Constant. It is well-known that the photophysical properties of Ru-terpy derivatives depend markedly on temperature due to the presence of thermally activated decay channels.⁷ For each derivative studied here, both Φ_{LUM} and τ_{LUM} increased progressively upon cooling

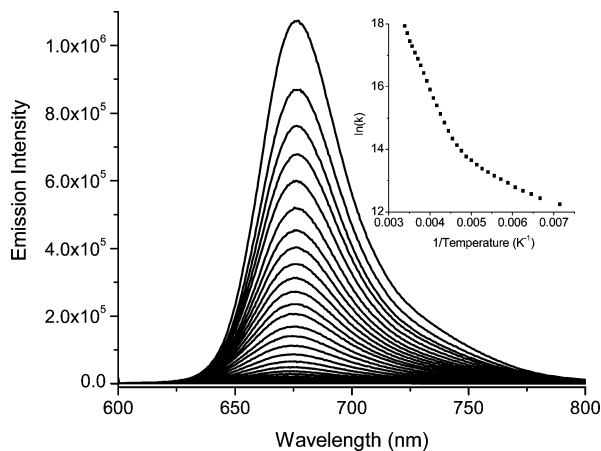


Figure 2. Effect of temperature (300 to 90 K) on the emission spectral profile recorded for **CE6** in butyronitrile. N.B. The intensity increases progressively with decreasing temperature. The inset shows a plot of the experimental data to eq 1.

the solution (Figure 2). There was no obvious change in the emission spectral profile and no shift in the emission maximum until the glass transition temperature was approached. Further cooling was accompanied by a 10 nm blue shift and a general narrowing of the emission band.²² The rate constant for nonradiative decay (k_{NR}) of the emitting triplet state was found to follow a modified Arrhenius-type expression of the form given as eq 1 (Figure 2).²³ Here, the lowest-energy triplet decays

$$k_{\text{NR}} = \left(\frac{1 - \Phi_{\text{LUM}}}{\tau_{\text{LUM}}} \right) = k_0 + k_A \exp\left(-\frac{E_A}{RT}\right) + k_B \exp\left(-\frac{E_B}{RT}\right) \quad (1)$$

with an activationless rate constant k_0 at low temperature but is coupled to two upper-lying triplet states. The first of these upper triplets, which is believed to be of MLCT character,²⁴ is reached by passing over a small barrier (E_A). This state decays (k_A) somewhat faster than the lowest-energy triplet. There is an additional triplet state, believed to be of metal-centered character,²⁵ which can be reached by crossing a more substantial barrier (E_B). This latter state decays rapidly (k_B) to re-form the ground state and is responsible for the poor emission yield found at ambient temperature.²⁶ The same analysis was carried out for each of the compounds, and the derived parameters are compiled in Table 1.

First, it should be stressed that 5 parameters have to be extracted from each set of data; attempts to fit the data to a 3-state model, thereby eliminating the upper-lying MLCT state, were unsatisfactory. Our analysis indicates a common set of parameters for interaction between the lowest-energy MLCT triplet and the upper-lying metal-centered (MC) state. Thus, k_B falls within a fairly narrow range and can be attributed to formation of the MC triplet since decay of this excited state is an internal conversion process involving a d–d transition and is likely to be very fast.²⁶ Formation of the MC state involves charge transfer from the π^* orbital localized on the ditopic ligand to an e_g orbital on the Ru^{III} center.²⁷ The activation barrier, E_B , associated with this process can be considered in terms of Marcus theory²⁸ to depend on the magnitude of the thermodynamic driving force and the reorganization energy accompanying charge transfer. The fact that both k_B and E_B are essentially independent of strap length can be taken as evidence that neither the driving force nor the reorganization energy is much affected by the dihedral angle around the connector. Indeed, there is no reason to suppose that the energy gap between MC and MLCT

TABLE 1. Parameters Derived from the Temperature-Dependent Photophysical Studies Carried Out in Deoxygenated Butyronitrile and the Dihedral Angles Computed for Energy-Minimized Geometries

compound	angle/ deg	$k_0/$ 10^4 s^{-1}	$k_A/$ 10^7 s^{-1}	$E_A/$ kJ mol^{-1}	$k_B/$ 10^{11} s^{-1}	$E_B/$ kJ mol^{-1}
C1	37	165	10.2	7.0	3.2	22.0
C2	55	210	16.0	7.2	3.5	22.9
C3	67	140	13.9	7.0	2.9	22.0
C4	94	5	10.9	7.2	3.0	22.3
CE4	122	165	16.6	7.1	3.7	23.0
CE5	125	170	6.4	7.0	3.6	22.8
CE5/Li⁺		6	6.5	7.3	3.6	22.7
CE5/Na⁺	83	2	8.3	6.9	3.5	22.9
CE5/K⁺	113	10	6.4	7.2	3.6	22.2
CE6	130	210	6.4	6.5	3.7	23.0
CE6/Na⁺	58	11	9.6	6.8	3.6	22.6
CE6/K⁺	62	7	6.4	6.7	3.5	22.4
R1	NA	6	2.1	8.6	200	20.3
R2	NA	3	5.0	10.0	160	32.0
R3	NA	2	5.1	9.3	125	28.5

triplets depends on the geometry of the bridging biphenyl unit. Furthermore, the reorganization energy for formation of the MC state is probably dominated by nuclear changes around the metal cation and is unlikely to show much sensitivity toward the geometry of the biphenyl group.

Within the precision of our data analysis, E_A and k_A likewise remain essentially independent of strap length. Here, the activation energy E_A corresponds to the barrier that must be crossed in order to populate the upper-lying MLCT triplet from the lowest-energy MLCT triplet state. It is considered that these two MLCT triplets differ by the amount of spin–orbit coupling, with the upper state possessing somewhat more singlet character.²⁹ Since the energy of the lowest-lying MLCT triplet is independent of strap length, it follows that the geometry of the bridge has no significant effect on the energy gap between these two triplet states. Both E_A and k_A remain comparable to values derived for the various reference compounds (Table 1).

In marked contrast, the derived k_0 values vary over a wide range, spanning from 2.0×10^4 to $2.1 \times 10^6 \text{ s}^{-1}$ (Table 1). This variation, which is well outside experimental error, cannot be assigned to changes in the amount of energy to be dissipated. It is interesting to note that those compounds having a cation bound at the crown ether derived strap exhibit particularly low k_0 values that are insensitive to the nature of the bound cation or strap length. The variation in k_0 found for the strapped compounds has little impact on the triplet lifetimes recorded at ambient temperature because of the competing activated processes. Our analysis requires that k_0 is independent of temperature, but this might be an approximation. Indeed, Meyer et al.³⁰ have shown that the rate of decay of MLCT triplet states should show a weak dependence on temperature due primarily to variations in entropy associated with frequency changes in solvent librations. Our analytical protocol would not detect such minor changes in rate.

$$k_0 = k_{\text{IND}} + k_{\text{DEP}} \sin^2(2\varphi) \quad (2)$$

These derived k_0 values can now be considered in terms of the geometry of the biphenyl-based bridge, as computed earlier from molecular mechanics and molecular dynamics simulations.^{14,31} The only obvious change among the various compounds is the structural distortion around the central biphenyl unit as imposed by the strap. The simplest way to represent this geometrical change is via the dihedral angle (φ) for the connecting C–C bond, which varies from 37° to 130° (Table

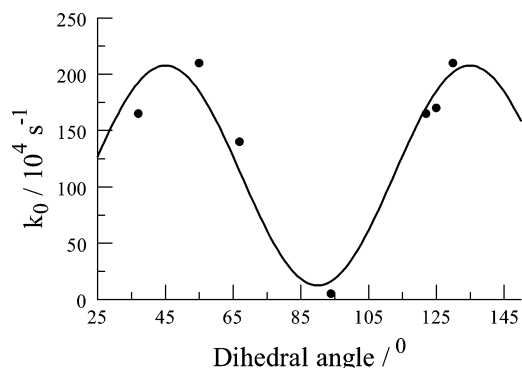


Figure 3. Effect of dihedral angle on the derived rate constant for nonradiative decay of the lowest-energy excited triplet state. The solid line is a nonlinear, least-squares fit to eq 2.

1). With the exception of the complexes possessing bound cations, there is a reasonably good correlation between k_0 and this dihedral angle (Figure 3). The correlation corresponds roughly to the form given as eq 2 where k_{IND} ($=8.7 \times 10^4 \text{ s}^{-1}$) refers to the angle-independent rate constant for nonradiative decay and k_{DEP} ($=2.3 \times 10^6 \text{ s}^{-1}$) is the analogous angle-dependent rate constant. The ratio of these rate constants ($k_{\text{DEP}}/k_{\text{IND}} = 26$) indicates that the conformation of the biphenyl unit can make a significant contribution to the overall decay rate. The maximum k_{DEP} value is observed when the two phenylene rings tend toward a mutual angle of 45° . The cation-bound complexes show but a very weak angle dependence which, within the precision of our data analysis, can be considered as being negligible.

It should also be emphasized that there is a 90-fold increase in k_0 between **C2**, where the dihedral angle is 55° , and the corresponding Ru-terpy complex lacking the strap. Indeed, k_0 values of $6.5 \times 10^4 \text{ s}^{-1}$ and $3.2 \times 10^4 \text{ s}^{-1}$, respectively, have been reported for ruthenium(II) bis-terpy (**R1**)²⁴ and for the mononuclear complex functionalized with a single phenylethynylene group at the 4'-position (**R2**).^{10g} For these two reference compounds, the change in k_0 reflects the amount of increased electron delocalization at the triplet level for **R2**. There is a further decrease in k_0 , and a corresponding increase in electron delocalization, for the extended reference compound **R3**. Interestingly, the derived value for k_{IND} , which reflects the rate at 0° , is somewhat higher than the k_0 value found for **R3** ($k_0 = 2.3 \times 10^4 \text{ s}^{-1}$) (Table 1), where the biphenyl unit is free to rotate. As will be suggested later, the increased k_0 found for the strapped derivatives might be a consequence of a coupled, low-frequency vibrational mode.

Emission Spectral Curve Fitting. Procedures now exist by which to analyze the emission spectrum in such a way as to extract useful information about the vibrational modes that promote nonradiative decay of the excited state.³² This analysis was carried out for the compounds under consideration here and over the full temperature range. The first step involves deconvolution of the reduced emission spectrum into the minimum number of Gaussian-shaped components of equal half-width (see Supporting Information).^{17,18} This analysis gives crude estimates for the energy gap (E_{00}) between 0,0 vibrational levels in excited and ground states and for the averaged magnitude of vibrational modes coupled to the decay process. Next, the entire emission spectrum is reconstituted using refined parameters and allowing for the relevant Huang–Rhys factors, S_{M} and S_{L} .¹⁹ It was found that the emission spectrum could be reproduced satisfactorily on the basis of a medium-frequency ($h\omega_{\text{M}}$) and a low-frequency ($h\omega_{\text{L}}$) vibrational mode being

TABLE 2. Parameters Extracted from the Curve Fitting Analysis and the Total Strain Energies for the Biphenyl-Based Connectors as Computed from AM1 Calculations for the Optimized Geometries

compound	E_{00} /cm ⁻¹	$h\omega_{\text{M}}$ / cm ⁻¹	$h\omega_{\text{L}}$ / cm ⁻¹	S_{M}	S_{L}	E_{STRAIN} / kJ mol ⁻¹
C1	14 820	1 390	738	0.13	0.36	2.2
C2	14 810	1 387	713	0.14	0.32	9.7
C3	14 815	1 400	818	0.11	0.34	2.6
C4	14 820	1 380	830	0.14	0.36	1.9
CE4	14 870	1 367	720	0.12	0.38	4.6
CE5	14 850	1 390	828	0.15	0.41	4.2
CE5/Li⁺	14 870	1 388	800	0.10	0.37	14.5
CE5/Na⁺	14 850	1 382	726	0.10	0.35	4.2
CE5/K⁺	14 860	1 350	800	0.10	0.38	5.1
CE6	14 825	1 400	780	0.11	0.32	2.6
CE6/Na⁺	14 825	1 386	800	0.08	0.35	6.7
CE6/K⁺	14 840	1 380	830	0.09	0.36	7.7

coupled to nonradiative decay, as indicated by eq 3. This analysis holds true over the full temperature range where the solvent remains fluid.

$$I(\nu) = \sum_{n_{\text{M}}}^7 \sum_{n_{\text{L}}}^7 \left\{ \left(\frac{E_{00} - n_{\text{M}}h\omega_{\text{M}} - n_{\text{L}}h\omega_{\text{L}}}{E_{00}} \right)^3 \left(\frac{S_{\text{M}}^{n_{\text{M}}}}{n_{\text{M}}!} \left(\frac{S_{\text{L}}^{n_{\text{L}}}}{n_{\text{L}}!} \right) \right) \exp \left(-4 \ln 2 \left(\frac{\nu - E_{00} + n_{\text{M}}h\omega_{\text{M}} + n_{\text{L}}h\omega_{\text{L}}}{\Delta\nu_{1/2}} \right)^2 \right) \right\} \quad (3)$$

In fitting the experimental data to eq 3, $I(\nu)$ is the normalized emission intensity at wavenumber ν , n_{M} and n_{L} are the vibrational quantum numbers for the averaged medium ($h\omega_{\text{M}}$) and low ($h\omega_{\text{L}}$) frequency acceptor modes, $\Delta\nu_{1/2}$ is the half-width of individual vibronic bands, and E_{00} is the energy gap for the 0,0 transition. The quantities S_{M} and S_{L} are the Huang–Rhys factors for medium- and low-frequency modes, respectively. The half-width depends on temperature, but most of the other parameters could be averaged over the entire temperature range (Table 2). The best fits to the experimental data result in an averaged $h\omega_{\text{M}}$ of 1385 cm^{-1} , which would correspond to a combination of C=C and C=N stretching modes, and an averaged $h\omega_{\text{L}}$ of 780 cm^{-1} . However, both frequencies tend to increase with increasing temperature (see Supporting Information); the variation in $h\omega_{\text{M}}$ is modest, but $h\omega_{\text{L}}$ shows a strong temperature effect; e.g. for **C4**, $h\omega_{\text{L}}$ varies from ca. 535 cm^{-1} at 90 K to 1020 cm^{-1} at 290 K. The temperature effect arises because there is a range of related vibrational frequencies associated with each mode rather than a single frequency as suggested by our analysis. With increasing temperature, the Boltzmann distribution moves steadily toward the higher-energy mean value. As such, the low-frequency mode is more sensitive to changes in temperature.³³ It is interesting to note that whereas the low-frequency vibrational mode was absent from emission spectra recorded for both **R1**²⁴ and **R2**,^{10g} an averaged $h\omega_{\text{L}}$ of 860 cm^{-1} had to be included for emission spectra recorded for **R3**. This behavior suggests that $h\omega_{\text{L}}$ is associated in some way with the biphenyl connector.

It is well established that the photophysical properties of certain ruthenium(II) poly(pyridine) complexes are sensitive to the nature of the surrounding solvent.³⁴ For **CE6**, however, it was found that the size of $h\omega_{\text{L}}$ was unaffected by changes in solvent polarity. There was more effect on the medium-frequency mode, which increased systematically, albeit slightly, with increasing solvent dielectric constant. This latter effect can be attributed to the fact that changes in the C=C and C=N stretching vibrations arise because of the difference in the

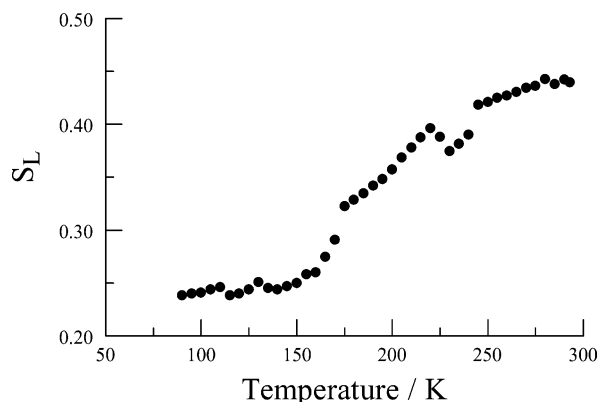


Figure 4. Effect of temperature on the derived S_L factor, obtained from fitting the emission spectrum of **C4** in deoxygenated butyronitrile.

charge-transfer character between ground and triplet states.³⁵ The lack of a significant solvent effect on $\hbar\omega_L$ implies that the low-frequency vibration is not associated with a charge-transfer process.

$$S_L = S_0 \coth\left(\frac{\hbar\omega_L}{2k_B T}\right) = S_0[2n_p(T) + 1]$$

$$n_p(T) = \left[\exp\left(\frac{\hbar\omega_L}{2k_B T}\right) - 1\right]^{-1} \quad (4)$$

As a consequence of the variation in $\hbar\omega_L$, there is a progressive increase in S_L with increasing temperature (Figure 4). A similar effect has been reported for the vibrational progression seen in the emission spectra of certain poly(*p*-phenylene vinylene) polymers.³⁶ Here, S_L increases with increasing temperature due to a decrease in the conjugation length caused by thermal disruption of extended planar geometries. For the complexes under investigation, the effect of temperature on S_L might also be explained in terms of thermal disorder around the biphenyl linker affecting the degree of electron–phonon coupling.³⁷ Thus, S_L can be related to the averaged low-frequency vibrational mode by way of eq 4, where S_0 is the coupling constant at 0 K and $n_p(T)$ is the thermal occupation number of phonon states. With increasing temperature, there will be increasing population of the upper-lying phonon states as thermal motion becomes more important. This effect will be modest for S_M but could be significant for S_L .³⁸

Role of the Bridging Biphenyl Unit. It should be noted that the strap length has no obvious effect on the derived E_{00} values and, as such, we can conclude that neither the triplet energy nor the conjugation length are affected significantly by changes in the length of the tether. Likewise, the absence of important polarity effects tends to rule out intramolecular charge-transfer effects as being primarily responsible for the variations in k_0 . There are no obvious indications that the degree of electron delocalization at the triplet level is related to the length of the strap. This latter situation would require leakage of electronic charge across the biphenyl group and would be affected by changes in the dihedral angle. In this case, the relevant angle would relate to the π -radical anion of the ditopic ligand, rather than the ground state as considered here. It should be noted that k_0 for the corresponding derivative lacking the dialkoxy strap, **R3**, is somewhat lower than for the compound having a single phenylene ring, **R2** (Table 1). This is consistent with electron delocalization extending over the second phenyl ring in the biphenyl group, provided the two rings can adopt a coplanar arrangement. The effect of extended π -electron de-

localization, however, is modest and does not account for the apparent angle dependence observed here. Instead, a more plausible explanation of the observed effects involves a contribution to the total nonradiative processes by torsional motions around the linking biphenyl unit, despite the remoteness of this group from the metal center. This possibility seems consistent with the observation that the enhancement in k_0 is curtailed upon binding a cation to the crown ether for both **CE5** and **CE6** since it is well-known that the resultant complex is considerably more rigid than the free ligand.³⁹ Molecular dynamics simulations have confirmed that, in addition to rotation of the phenylene rings, there is considerable fluctuation of the strap at ambient temperature.¹⁴

Taking account of both low- and medium-frequency vibrational modes, the variation of k_0 among the compounds can be considered in terms of the Englman–Jortner energy-gap law as outlined in eq 5. Here, the electronic states are mixed by

$$k_0 = \frac{\beta_0}{\sqrt{\hbar\omega_M \Delta E}} e^{-S_M} e^{-\gamma E_{00}/(\hbar\omega_M)} e^{\kappa}$$

$$\kappa = \left(\frac{\gamma + 1}{\hbar\omega_M}\right)^2 \frac{2(\Delta\nu_{1/2})^2}{16 \ln 2}$$

$$\Delta\nu_{1/2} = \left[S_L (\hbar\omega_L)^2 \coth\left(\frac{\hbar\omega_L}{2k_B T}\right) + 2k_B T \chi_0 \right] (8 \ln 2)$$

$$\gamma = \ln \left[\frac{E_{00}}{S_M \hbar\omega_M} \right] - 1$$

$$\beta_0 = C^2 \omega \sqrt{\frac{\pi}{2}} \quad (5)$$

coupling to averaged vibrations that promote breakdown of the orthogonality of adiabatic Born–Oppenheimer states. The term β_0 refers to the vibrationally induced electronic coupling parameter, where C is the coupling matrix element and ω is the angular frequency of the promoting mode(s). The solvent reorganization energy χ_0 is small. Under these conditions, the apparent angle dependence found for nonradiative decay of these binuclear complexes stems from variations in β_0 . Since k_0 relates to the low-temperature regime, the geometry of the bridging biphenyl unit will approach that of the lowest-energy conformation where the dihedral angle is set by the length of the tether. Usually, the low-frequency mode has little effect on k_0 and the rate is set by factors related to the medium-frequency vibrational mode, but this is not the case for these strapped derivatives. In principle, all the parameters can be derived from emission spectral curve fitting, except for β_0 . It is also clear that k_0 should depend somewhat on temperature.³⁰

The results lead to two important findings. First, β_0 depends on the geometry of the appended biphenyl moiety. It should be emphasized, however, that the strap distorts the biphenyl group and that the central dihedral angle is only one indicator of this structural disruption. In addition, there are modest changes in the shape of the biphenyl group as shown by Figure 5. A better indicator of the total structural distortion imposed by the strap might be obtained from the overall strain energy (E_{STRAIN}) as computed by comparing the heat of formation of the strapped bridge with that of a biphenyl derivative having the same torsion angle but free from structural distortion. There is no obvious relationship between k_0 and E_{STRAIN} , as calculated for the corresponding ground-state structures (Table 2). This finding

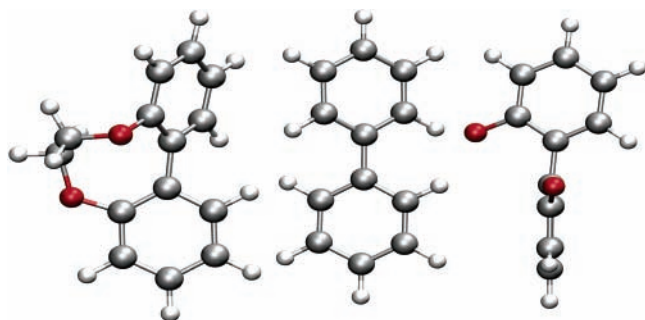


Figure 5. Variation in the geometry of the biphenyl group as imposed by the tethering strap. Energy-minimized structures are shown for **C2** (left), biphenyl (center), and 2,2'-dimethoxybiphenyl (right); in the latter case the methyl groups have been omitted for clarity of presentation.

suggests that the important property coupled to nonradiative decay is internal rotation of the biphenyl group and geometric modification of the entire biphenyl unit.

Second, binding a cation at the cavity provided by the crown ether dampens out the dependence of k_0 on structural facets of the bridging group. This has the effect of removing the low-frequency vibrational mode and thereby enhancing the triplet lifetime. Molecular dynamics simulations are consistent with the cation binding to the O atoms furthest from the biphenyl nucleus.¹⁴ The cation complex is thereby rigidified and has less effect on the shape of the biphenyl group.

Concluding Remarks

This work has shown that the rate of nonradiative decay of the triplet MLCT state is affected by remote substituents that do not impose any significant electronic effects. Quenching can be attributed to the coupling of a low-frequency vibrational mode to nonradiative decay. The extent of such coupling appears to correlate with the dihedral angle of the bridging biphenyl unit, as imposed by attaching a tethering chain around the 2,2'-positions of the biphenyl linker. This gives rise to a tenuous relationship between the rate constant and the torsion angle of the central C–C bond. An unexpected feature of this behavior is that cations included in the macrocycle provided by certain straps inhibit the quenching effect. This is quite a remarkable effect and serves to illustrate how minor changes in the structure of such metal complexes can exert profound changes in the photophysical properties.

Acknowledgment. We thank the EPSRC (GR/S00088/01) and the University of Newcastle for financial support of this work. The loan of precious metal salts by Johnson-Matthey Plc is gratefully acknowledged. We also thank the EPSRC mass spectrometry service at Swansea.

Supporting Information Available: Synthetic details for **R3**, a typical example of the analytical protocol used to deconvolute emission spectra, and collated data for the effect of temperature on the magnitude of $\hbar\omega_L$ and $\hbar\omega_M$. This material is available free of charge via the Internet at <http://pubs.acs.org>.

References and Notes

- Englman, R.; Jortner, J. *Mol. Phys.* **1970**, *18*, 145.
- Anderson, P. A.; Keene, F. R.; Meyer, T. J.; Moss, J. A.; Strouse, G. F.; Treadway, J. A. *Dalton Trans.* **2002**, 3820.
- (a) Bixon, M.; Jortner, J.; Cortes, J.; Heitele, H.; Michel-Beyerle, M. E. *J. Phys. Chem.* **1994**, *98*, 7289. (b) Chynwat, V.; Frank, H. A. *Chem. Phys.* **1995**, *194*, 237.
- (4) Helenius, V.; Monshouwer, R.; von Grondelle, R. *J. Phys. Chem.* **1997**, *101*, 10554.
- (5) (a) Caspar, J. V.; Meyer, T. J. *Inorg. Chem.* **1983**, *22*, 2444. (b) Allen, G. H.; White, R. P.; Rillema, D. P.; Meyer, T. J. *J. Am. Chem. Soc.* **1984**, *106*, 2613. (c) Barqawi, K. R.; Llobet, A.; Meyer, T. J. *J. Am. Chem. Soc.* **1988**, *110*, 7751. (d) Lumpkin, R. S.; Kober, M. E.; Worl, L. A.; Murtaza, Z.; Meyer, T. J. *J. Phys. Chem.* **1990**, *94*, 239. (e) Rillema, D. P.; Blanton, C. B.; Shaer, R. J.; Jackman, D. C.; Boldaji, M.; Brundy, S.; Worl, L. A.; Meyer, T. J. *Inorg. Chem.* **1992**, *31*, 1600.
- (6) (a) Harrigan, R. W.; Hager, G. D.; Crosby, G. A. *Chem. Phys. Lett.* **1973**, *21*, 487. (b) Allsop, S. R.; Cox, A.; Jenkins, S. H.; Kemp, T. J.; Tunstall, S. M. *Chem. Phys. Lett.* **1976**, *43*, 135. (c) Islam, A.; Ikeda, N.; Nozaki, K.; Ohno, T. *Chem. Phys. Lett.* **1996**, *263*, 209.
- (7) (a) Thompson, D. W.; Wishart, J. F.; Brunschwigg, B. S.; Sutin, N. *J. Phys. Chem. A* **2001**, *105*, 8117. (b) Bhasikuttan, A. C.; Suzuki, M.; Nakashima, S.; Okada, T. *J. Am. Chem. Soc.* **2002**, *124*, 8398.
- (8) Benniston, A. C.; Harriman, A.; Li, P.; Sams, C. A. *J. Phys. Chem. A* **2005**, *109*, 2302.
- (9) Schoonover, J. R.; Bates, W. D.; Meyer, T. J. *Inorg. Chem.* **1995**, *34*, 6421.
- (10) (a) Grosshenny, V.; Harriman, A.; Romero, F. M.; Ziessel, R. *J. Phys. Chem.* **1996**, *100*, 17472. (b) Damrauer, N. H.; Boussie, T. R.; Devenney, M.; McCusker, J. K. *J. Am. Chem. Soc.* **1997**, *119*, 8253. (c) Hammarstrom, L.; Barigelli, F.; Flamigni, L.; Indelli, M. T.; Armaroli, N.; Calogero, G.; Guardigli, M.; Sour, A.; Collin, J.-P.; Sauvage, J.-P. *J. Phys. Chem. A* **1997**, *101*, 9061. (d) Damrauer, N. H.; McCusker, J. K. *J. Phys. Chem. A* **1999**, *103*, 8440. (e) Walters, K. A.; Premvardhan, L. L.; Liu, Y.; Peteanu, L. A.; Schanze, K. S. *Chem. Phys. Lett.* **2001**, *339*, 255. (f) Browne, W. R.; Coates, C. G.; Brady, C.; Matousek, P.; Towrie, M.; Botchway, S. W.; Parker, A. W.; Vos, J. G.; McGarvey, J. J. *J. Am. Chem. Soc.* **2003**, *125*, 1706. (g) Benniston, A.; Chapman, G.; Harriman, A.; Mehrabi, M.; Sams, C. A. *Inorg. Chem.* **2004**, *43*, 4227.
- (11) Benniston, A. C.; Harriman, A.; Li, P.; Sams, C. A. *Phys. Chem. Chem. Phys.* **2004**, *6*, 875.
- (12) Benniston, A. C.; Harriman, A.; Li, P.; Patel, P. V.; Sams, C. A. *Phys. Chem. Chem. Phys.* **2005**, *7*, 3677.
- (13) Benniston, A. C.; Harriman, A.; Li, P.; Sams, C. A. *Tetrahedron Lett.* **2003**, *44*, 4167.
- (14) Benniston, A. C.; Harriman, A.; Patel, P. V.; Sams, C. A. *Eur. J. Org. Chem.* **2005**, 4685.
- (15) Benniston, A. C.; Harriman, A.; Li, P.; Sams, C. A.; Ward, M. D. *J. Am. Chem. Soc.* **2004**, *126*, 13630.
- (16) Demas, J. N.; Crosby, G. A. *J. Am. Chem. Soc.* **1971**, *93*, 2841.
- (17) Barqawi, K. R.; Murtaza, Z.; Meyer, T. J. *J. Phys. Chem.* **1991**, *95*, 47.
- (18) Treadway, J. A.; Loeb, B.; Lopez, R.; Anderson, P. A.; Keene, F. R.; Meyer, T. J. *Inorg. Chem.* **1996**, *35*, 2242.
- (19) Smedarchina, Z.; Fernandez-Ramos, A.; Siebrand, W. *J. Comput. Chem.* **2001**, *22*, 787.
- (20) (a) Harriman, A.; Ziessel, R. *Chem. Commun.* **1996**, 1707. (b) Harriman, A.; Ziessel, R. *Coord. Chem. Rev.* **1998**, *171*, 331. (c) Ziessel, R.; Hissler, M.; El-Ghayoury, A.; Harriman, A. *Coord. Chem. Rev.* **1998**, *178*, 1251.
- (21) (a) Grosshenny, V.; Harriman, A.; Ziessel, R. *Angew. Chem., Int. Ed. Engl.* **1995**, *34*, 1100. (b) Hissler, M.; El-ghayoury, A.; Harriman, A.; Ziessel, R. *Angew. Chem., Int. Ed.* **1998**, *37*, 1717. (c) El-ghayoury, A.; Harriman, A.; Khatyr, A.; Ziessel, R. *J. Phys. Chem. A* **2000**, *104*, 1512. (d) El-ghayoury, A.; Harriman, A.; Ziessel, R. *J. Phys. Chem. A* **2000**, *104*, 7906. (e) Harriman, A.; Mayeux, A.; De Nicola, A.; Ziessel, R. *Phys. Chem. Chem. Phys.* **2002**, *4*, 2229.
- (22) Beley, M.; Collin, J.-P.; Sauvage, J.-P.; Sugihara, H.; Heisel, F.; Miehé, A. *J. Chem. Soc., Dalton Trans.* **1991**, 3157.
- (23) Sacksteder, L. A.; Lee, M.; Demas, J. N.; DeGraff, B. A. *J. Am. Chem. Soc.* **1993**, *115*, 8230.
- (24) Amini, A.; Harriman, A.; Mayeux, A. *Phys. Chem. Chem. Phys.* **2004**, *6*, 1157.
- (25) (a) Kirchoff, J. R.; McMillin, D. R.; Marnot, P. A.; Sauvage, J.-P. *J. Am. Chem. Soc.* **1985**, *107*, 1138. (b) Hecker, C. R.; Gushurst, A. K. I.; McMillin, D. R. *Inorg. Chem.* **1991**, *30*, 538. (c) Coe, B. J.; Thompson, B. W.; Culbertson, C. D.; Schoonover, J. R.; Meyer, T. J. *Inorg. Chem.* **1995**, *34*, 3385.
- (26) Sauvage, J.-P.; Collin, J.-P.; Chambron, J.-C.; Guillerez, S.; Coudret, C.; Balzani, V.; Barigelli, F.; De Cola, L.; Flamigni, L. *Chem. Rev.* **1994**, *94*, 993.
- (27) Islam, A.; Ikeda, N.; Yoshimura, A.; Ohno, T. *Inorg. Chem.* **1998**, *37*, 3093.
- (28) Marcus, R. A. *Annu. Rev. Phys. Chem.* **1964**, *15*, 155.
- (29) (a) Kober, E. M.; Meyer, T. J. *Inorg. Chem.* **1984**, *23*, 3877. (b) Sykora, M.; Kincaid, J. R. *Inorg. Chem.* **1995**, *34*, 5852.
- (30) Claude, J. P.; Meyer, T. J. *J. Phys. Chem.* **1995**, *99*, 51.
- (31) The molecular mechanics calculations were carried out for systems in vacuo whereas the experimental studies refer to fluid solution. It seems likely that the surrounding solvent will dampen internal motions, such that the range of angles accessible to any given conformation might be decreased relative to the gas phase. The energy-minimized geometries, however, are

unlikely to change significantly. This situation has been demonstrated for the hydrocarbon straps by carrying out computations in a reservoir of acetonitrile molecules.

(32) Chang, R.; Hsu, J. H.; Fann, W. S.; Liang, K. K.; Chang, C. H.; Hayashi, M.; Yu, J.; Lin, S. H.; Chang, E. C.; Chuang, K. R.; Chen, S. A. *Chem. Phys. Lett.* **2000**, *317*, 142.

(33) Borges, C. A. M.; Marletta, A.; Faria, R. M.; Guimaraes, F. E. G. *Braz. J. Phys.* **2004**, *34*, 590.

(34) Caspar, J. V.; Meyer, T. J. *J. Am. Chem. Soc.* **1983**, *105*, 5583.

(35) Xie, P.; Chen, Y.-J.; Uddin, M. J.; Endicott, J. F. *J. Phys. Chem. A* **2005**, *109*, 4671.

(36) (a) Rossi, G.; Chance, R. R.; Silbey, R. J. *J. Chem. Phys.* **1989**, *90*, 7594. (b) Lhost, O.; Brédas, J. L. *J. Chem. Phys.* **1992**, *96*, 5279. (c) Yaliraki, S. N.; Silbey, R. J. *J. Chem. Phys.* **1996**, *104*, 1245. (d) Wood, P.; Samuel, I. D. W.; Schrock, R.; Christensen, R. L. *J. Chem. Phys.* **2001**, *115*, 10955.

(37) Chang, T.-C.; Chou, S.-H.; Li, H.-W.; Lin, S.-H. *J. Chem. Phys.* **1993**, *99*, 2781.

(38) Lin, S.-H. *J. Chem. Phys.* **1976**, *65*, 1053.

(39) Gokel, G. W.; Leevy, W. M.; Weber, M. E. *Chem. Rev.* **2004**, *104*, 2723.